AGU PUBLICATIONS

Geophysical Research Letters

RESEARCH LETTER
10.1002/2017GL072920

**Key Points:**
- The 2015-2016 Eastern Pacific El Niño reached a record-breaking sea surface temperature anomalies in the Central Pacific region
- An extremely early stratospheric final warming occurred in early March 2016, with impacts over the North Atlantic and Europe
- When accompanied by early stratospheric final warmings, central Pacific El Niño events have tropospheric effects in late winter and spring

**Correspondence to:**
F. M. Palmeiro,
fm.palmeiro@fis.ucm.es

**Citation:**
Palmeiro, F. M., M. Iza, D. Barriopedro, N. Calvo, and R. García-Herrera (2017), The complex behavior of El Niño winter 2015–2016, *Geophys. Res. Lett.*, *44*, 2902–2910, doi:10.1002/2017GL072920.

Received 8 FEB 2017
Accepted 8 MAR 2017
Accepted article online 15 MAR 2017
Published online 25 MAR 2017



# The complex behavior of El Niño winter 2015–2016

**F. M. Palmeiro[1], M. Iza[1], D. Barriopedro[1,2], N. Calvo[1], and R. García-Herrera[1,2]**

[1]Dpto Física de la Tierra II, Facultad de Ciencias Físicas, Universidad Complutense de Madrid, Madrid, Spain, [2]Instituto de Geociencias, CSIC-UCM, Madrid, Spain

**Abstract** This paper examines the outstanding characteristics of the strong 2015–2016 El Niño (EN) winter and its impact over the European region through the stratosphere. Despite being classified as a strong eastern Pacific (EP) EN event, our analysis reveals an anomalous behavior, with some signatures that are more typical of central Pacific (CP) EN events instead. They include (i) a record-breaking value of the CP index, (ii) a stronger polar vortex in early and midwinter, due to reduced upward wave activity and a weakened Aleutian low, and (iii) the occurrence of one of the earliest stratospheric final warmings (SFWs) on record, which are more prone to occur during CP-EN. Following the SFW, a stratospheric influence on the Euro-Atlantic sector is reported in spring, with persistent Greenland blocking resulting in extreme precipitation over some southern European regions. Results highlight the importance of considering early SFWs as mediators of El Niño teleconnections.

## 1. Introduction

The winter of 2015–2016 was characterized by one of the strongest El Niño (EN) events on record. Different from other strong episodes as those during 1982–1983 and 1997–1998 winters, the largest sea surface temperature anomalies (SSTAs) of EN 2015–2016 (EN15/16) were not confined to the east Pacific Ocean [*Parker et al*., 2015] but extended toward the central Pacific and west of the dateline [*L'Heureux et al*., 2016]. Thus, it showed SSTA signatures of both eastern Pacific (EP) and central Pacific (CP) EN events. The type of EN event is a key for polar stratospheric responses in the Northern Hemisphere (NH). While the NH polar vortex warms and weakens during EP-EN events [e.g., *García-Herrera et al*., 2006], a robust colder polar stratosphere and stronger polar vortex occurs during CP-EN winters in the absence of stratospheric sudden warmings (SSWs) [*Iza and Calvo*, 2015]. This is opposite to the behavior found for EP-EN regardless of the occurrence of SSWs. In addition, the EP-EN related polar stratospheric anomalies propagate downward and impact surface climate in the North Atlantic European (NAE) region [*Manzini et al*., 2006; *Bell et al*., 2009; *Cagnazzo and Manzini*, 2009; *Ineson and Scaife*, 2009]. However, there are no evidences of a robust NAE response to CP-EN events [*Garfinkel et al*., 2013; *Iza and Calvo*, 2015, and references therein].

Although previous studies have reported a modulating role of SSWs in the EN signal, less attention has been paid to other stratospheric phenomena perturbing the polar vortex, such as stratospheric final warmings (SFWs). They imply a permanent reversal of the stratospheric circulation, thus marking the end of the winter season in both hemispheres [*Black et al*., 2006]. Interestingly, EN15/16 was accompanied by the earliest SFW of the last decades, registered on 6 March, about a month earlier than the average onset date of SFWs (April). Regardless the occurrence of EN events, many authors have noted that tropospheric responses to early SFWs differ from those to late SFWs [e.g., *Ren and Hu*, 2014]. The effects are particularly observed over the NAE region [*Black et al*., 2006; *Gimeno et al*., 2007] and in relation to the storm track activity [*Ayarzagüena and Serrano*, 2009; *Hardiman et al*., 2011]. In this sense, anomalous precipitation over southern Europe occurred in the spring of 2016, following the SFW on 6 March, with departure values reaching about 150% of the totals over western Iberia.

The unusual characteristics of EN15/16, together with the occurrence of an extremely early SFW and the increased precipitation over southern Europe, motivate our study. Note that EN15/16 might have also influenced the stratospheric zonal winds in the tropics and thus the quasi-biennial oscillation (QBO), which showed an unprecedented transition to its easterly phase [*Newman et al*., 2016; *Osprey et al*., 2016]. Although a deeper analysis on this link is out of the scope of this paper, the unusual disruption of the QBO adds to the exceptional behavior of the EN15/16 winter. Our aim is to explore the stratospheric pathway of the anomalous EN15/16, its relation with the early SFW and the following surface impacts in the NAE region.

## 2. Data and Methods

November to February monthly SSTs have been obtained from the Met Office Hadley Centre (HadISST1) for the Niño3 (N3) (5°N–5°S, 150°W–90°W) and Niño4 (N4) (5°N–5°S, 160°E–150°W) regions at 1° × 1° horizontal resolution [*Rayner et al*., 2003]. Monthly mean and daily mean atmospheric data were obtained from the European Center for Medium-Range Weather Forecasts (ECMWF) ERA-40 reanalysis for 1957–1979 and ERA-Interim for 1979–2016 [*Uppala et al*., 2005; *Dee et al*., 2011]. Note that no other data set extending up to the upper stratosphere was available for 2015–2016 at the time of this study. Anomalies were computed for each time step (daily or monthly) by subtracting its long-term climatology over the period 1981–2010. The statistical significance of the results was assessed with a 1000-trial Monte Carlo test.

Throughout the paper, EN15/16 is compared with EP-EN and CP-EN composites during the period 1958–2015. Following *Iza and Calvo* [2015], N3 and N4 El Niño indices are calculated as the standardized SSTA previously detrended, EP-EN winters are identified whenever N3 exceeds 0.5 standard deviations (SD) and N3 is larger than 0.1 times the N4 value. Similarly, CP-EN winters are defined whenever N4 exceeds 0.5 SD, and N4 is larger than 0.1 times the N3 value. The composites include 6 EP-EN winters (1965–1966, 1972–1973, 1976–1977, 1982–1983, 1991–1992, 1997–1998) and 12 CP-EN winters (1968–1969, 1977–1978, 1979–1980, 1987–1988, 1990–1991, 1994–1995, 2002–2003, 2003–2004, 2004–2005, 2006–2007, 2009–2010, and 2014–2015). Note that EN15/16 is herein analyzed independently.

SSWs and SFWs are often characterized by a pronounced warming of the NH polar stratosphere and the breakdown of the polar vortex [e.g., *Matsuno*, 1971]. They have been identified as a reversal of the zonal mean zonal wind at 10 hPa and at any latitude between 55°N and 70°N during the extended NH winter season from November to March [*Palmeiro et al*., 2015]. The first day of easterlies is referred to as the onset date. The event is considered a SSW if the zonal mean zonal wind returns to westerlies for at least 10 consecutive days before 30 April, otherwise it is classified as a SFW [*Charlton and Polvani*, 2007]. We consider early SFWs as those occurring before 13 March, which is the 10th percentile of the SFW onset date distribution.

The Northern Annular Mode (NAM) index measures the strength of the polar vortex (jet stream) in the stratosphere (troposphere), and it is a powerful metric to characterize the stratosphere-troposphere coupling [e.g., *Baldwin and Dunkerton*, 2001]. It has been computed on a daily basis and at each pressure level as the standardized first principal component of the zonal mean geopotential height anomalies north of 20°N. To further characterize the anomalous tropospheric conditions of the EN15/16 winter over the NAE sector, we diagnosed the occurrence of atmospheric blocking episodes as large-scale, quasi-stationary systems with daily geopotential height anomalies at 500 hPa reversing the meridional gradient and persisting at least 5 days [*Barriopedro et al*., 2010]. Monthly liquid precipitation totals over land were derived from the Global Precipitation Climatology Centre database [*Schneider et al*., 2015a, 2015b] at 1° × 1° spatial resolution.

## 3. Results

Figure 1 shows the monthly evolution of the Pacific SSTAs for the 2015–2016 winter, together with the composites of EP-EN and CP-EN winters. During EP-EN (Figure 1, middle row), the traditional SSTA pattern is well reproduced, with tropical warm SSTAs extending from the coasts of Ecuador and Peru. The SSTA pattern for CP-EN (Figure 1, bottom row) shows a westward extension of the anomalies, with maximum values in the Central Pacific and significant positive anomalies crossing the dateline. The weaker SSTAs of CP-EN are not an artifact of the thresholds chosen for the selection of EN events (not shown) but a well-established signature of this EN flavor [e.g., *Ashok et al*., 2007; *Zubiaurre and Calvo*, 2012]. EN15/16 (Figure 1, top row) is a combination of both types of events. During most of the winter, large SSTAs were observed in the Eastern Pacific, and hence, the EN15/16 event is classified as EP-EN (N3 = 2.2 SD; N4 = 1.8 SD), being the third strongest on the 59 year record. However, warm anomalies also extended across the dateline throughout the winter reaching the central Pacific by January. In fact, the SSTAs in the CP region reached the largest value on record and exceeded by more than 0.3 SD the previous strongest N4 value.

We next examine the NH stratospheric responses to EN15/16 considering the monthly evolution of the zonal mean temperature anomalies in a latitude-height cross section in comparison with the composite behavior of EP-EN and CP-EN events (Figure 2). EN15/16 displayed an anomalous stratospheric polar cooling from December to February with warming above, which reflects a strengthening of the polar vortex (not shown).

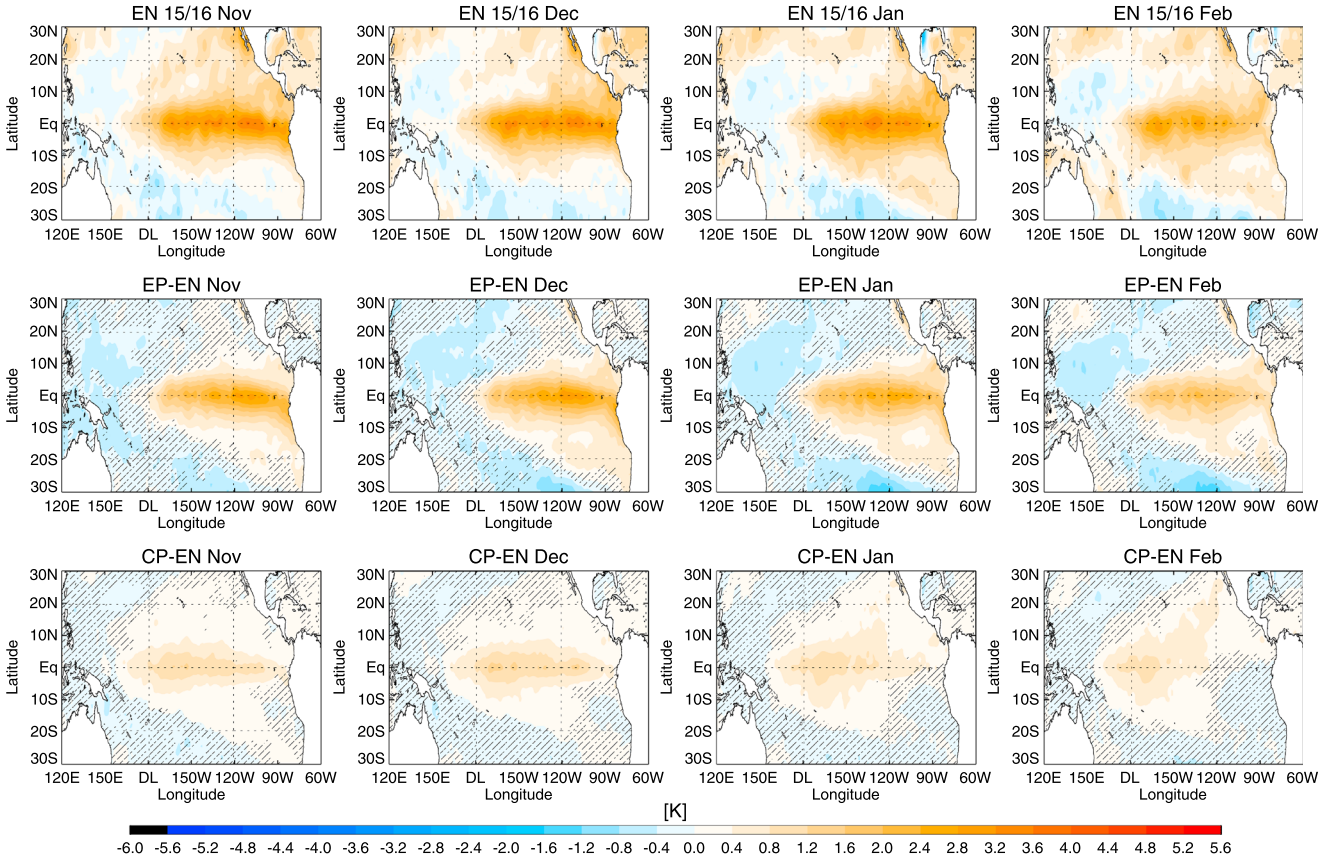


**Figure 1.** Longitude-latitude monthly SSTAs from November to February for (top row) EN15/16, (middle row) EP-EN and (bottom row) CP-EN. In Figure 1 (middle and bottom rows), stippling indicates where the signal is not significant at the 90% confidence level.

Interestingly, this response resembles that of CP-EN events without SSWs (Figure 2, middle row [see also *Iza and Calvo*, 2015]) and it is the opposite of that associated with EP-EN winters until February (Figure 2, bottom row).

The observed colder and stronger polar vortex was consistent with reduced upward wave activity in November and December 2015 (Figure 3, bottom row) and an anomalously weak Aleutian low in November (Figure 3, top row). This behavior is also the opposite of EP-EN events [*Manzini et al*., 2006], and it is in good agreement with that observed during CP-EN winters without SSWs [*Iza and Calvo*, 2015, Figure 3d]. Thus, despite being cataloged as an EP-EN, the extratropical tropospheric responses and the polar stratospheric signatures of EN15/16 resembled those of a CP-EN winter, confirming the complex behavior of this event. The cold and strong polar vortex in midwinter was replaced by an anomalous warming and weaker polar vortex in March 2016 (Figure 2), which agrees with a deeper Aleutian low and intensified upward propagation of stationary wave number 1 in January and February (Figure 3). Note also that the late-winter warming of the polar stratosphere is also in better agreement with CP-EN than with EP-EN events (Figure 2).

Previous studies have shown that the occurrence of SSWs modulates the EP-EN and CP-EN signals in the stratosphere [*Cagnazzo and Manzini*, 2009; *Ineson and Scaife*, 2009; *Iza and Calvo*, 2015]. *Hu et al*. [2014a] already showed that early SFWs are more probable to occur in winters without SSWs. Further analyses on daily time scales (not shown) show an abrupt stratospheric warming at the time of the SFW onset, confirming that the monthly mean anomalies in March 2016 were largely due to the occurrence of the SFW. This implies that, in addition to SSWs, early SFWs can also have a fingerprint on the stratospheric signal of EN. Interestingly, four other early SFWs coincided with CP-EN events in the observational record, while only one occurred during EP-EN winters. Thus, the rate of occurrence of early SFWs is 0.33 during CP-EN (which is significantly higher than that expected from the climatology at $p < 0.05$ after a binomial test), compared to 0.17 during EP-EN (not significant at $p < 0.10$). This suggests that early SFWs are more prone to occur during CP-EN, partially explaining the late-winter warming associated with these EN events (Figure 2).

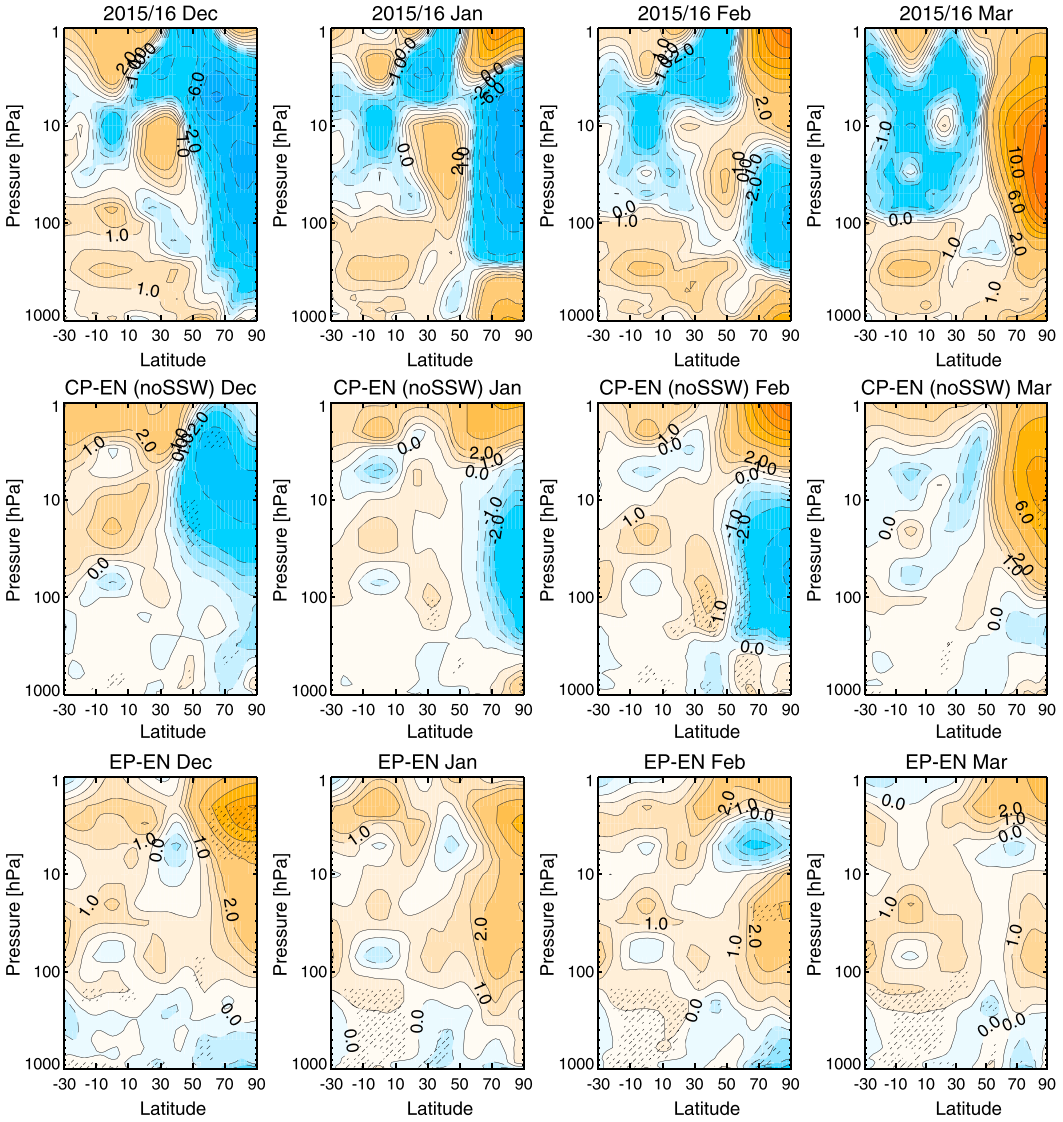


**Figure 2.** Latitude-pressure cross section of monthly zonal mean temperature anomalies from December to March for (top row) 2015–2016 winter, (middle row) CP-EN winters without SSWs, and (bottom row) EP-EN winters. Solid (dashed) contours denote positive (negative) anomalies. In Figure 2 (middle and bottom rows), stippling indicates the region where the signal is statistically significant at the 90% confidence level.

While the overall evolution of the stratospheric anomalies in EN15/16 agrees well with that of CP-EN, the warming in March 2016 extended well into the troposphere (Figure 2), thus suggesting a stratosphere-troposphere coupling response to the 2016 SFW. To further address it, we analyze the evolution of the polar vortex around the onset date of that SFW in Figure 4 (top), which shows the height-time cross section of the daily NAM index. After the 2016 SFW (day 0), there is a downward propagation of the negative NAM anomalies into the troposphere and the surface for several weeks. This stratosphere-troposphere coupling is similar to that reported for SSWs [*Baldwin and Dunkerton*, 2001], and both are stronger than that for all SFWs from 1958 to 2015 (Figure 4, middle). Previous studies have also reported a distinctive and stronger coupling of early SFWs [*Ayarzagüena and Serrano*, 2009; *Ren and Hu*, 2014]. To further stress the CP-EN-like stratospheric behavior of EN15/16, we have computed the composite of early SFWs during CP-EN events (Figure 4, bottom). The results show that, when accompanied by early SFWs, CP-EN winters show significant negative NAM anomalies propagating into the troposphere and persisting there for several weeks but the same is not observed in CP-EN without early SFWs (not shown), which could explain the absence of robust significant tropospheric responses to CP-EN in previous studies where CP-EN events are considered altogether. Thus,

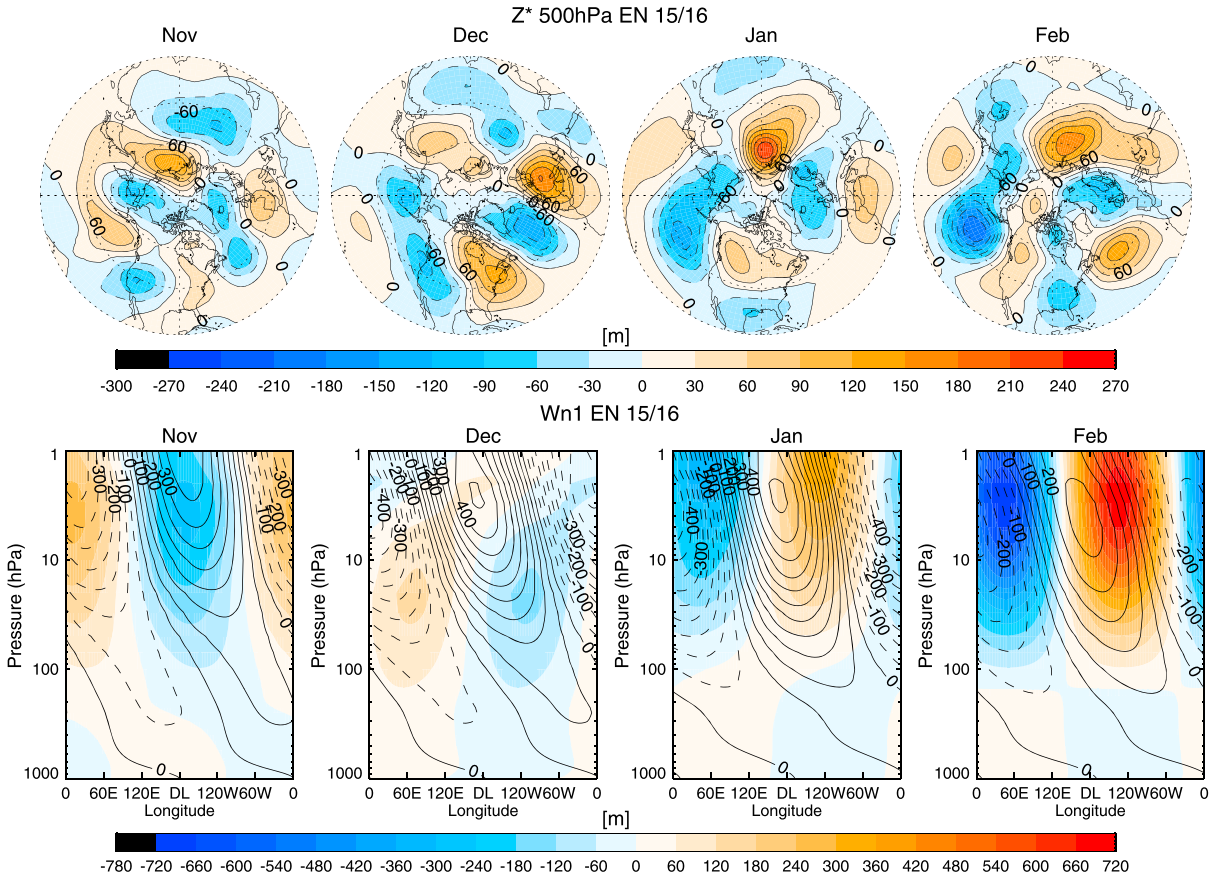


**Figure 3.** November to February evolution of (top row) Northern Hemisphere longitude-latitude eddy geopotential height anomalies at 500 hPa and (bottom row) longitude-pressure cross sections of the wave number 1 component of 45°N–75°N geopotential height anomalies (color shading) for EN15/16 winter. Solid (dashed) contours denote positive (negative) anomalies (Figure 3, top row). Solid (dashed) line contours denote positive (negative) climatological values (interval of 50 m) (Figure 3, bottom row).

the enhanced occurrence of early SFWs during CP-EN winters (Figure 4, bottom) provides evidences of a link between CP-EN and NAE conditions.

Finally, the tropospheric responses to the negative NAM anomalies associated with the 2016 SFW are explored over the NAE region. Overall, negative NAM values are associated with an equatorward shift of the storm tracks [*Thompson and Wallace*, 1998] and subsequent changes in precipitation. Figure 5 (top left) shows the seasonal (March to May 2016) anomalies of Z500 (contours) including approximately the 90 day period after the SFW. The negative height anomalies over southwestern Europe indicate a high frequency of low-pressure systems at ~50°N (southward from the typical latitude of the maximum storm-track activity). Accordingly, southern Europe and large areas of the Mediterranean experienced above-normal precipitation (Figure 5, shading), with seasonal mean departure values reaching ~150% of the totals over western Iberia and the Balkans, locally exceeding the 95th percentile of the spring distribution. The large positive height anomalies over the Atlantic extend from the midlatitudes to Greenland and are reminiscent of blocking patterns, which divert the paths of extratropical low-pressure systems toward southern latitudes. In fact, the 2016 spring blocking activity was above normal over Greenland (Figure 5, right column), with an absolute blocking activity of ~20%. This increased blocking activity mainly occurred in mid-March and April (not shown), in agreement with the strongest NAM tropospheric signal seen after the SFW (Figure 4). The connection between polar stratospheric circulation anomalies and Greenland blocking has been previously documented [e.g., *Barriopedro and Calvo*, 2014, and references therein]. In particular, enhanced activity of Greenland blocking has been related to negative NAM phases [*Davini et al*., 2014], a southward shift of the eddy-driven Atlantic jet stream [*Woollings et al*., 2010], and above-normal precipitation over the Mediterranean region [*Sousa et al*., 2016], as observed in 2016. The comparison of the tropospheric

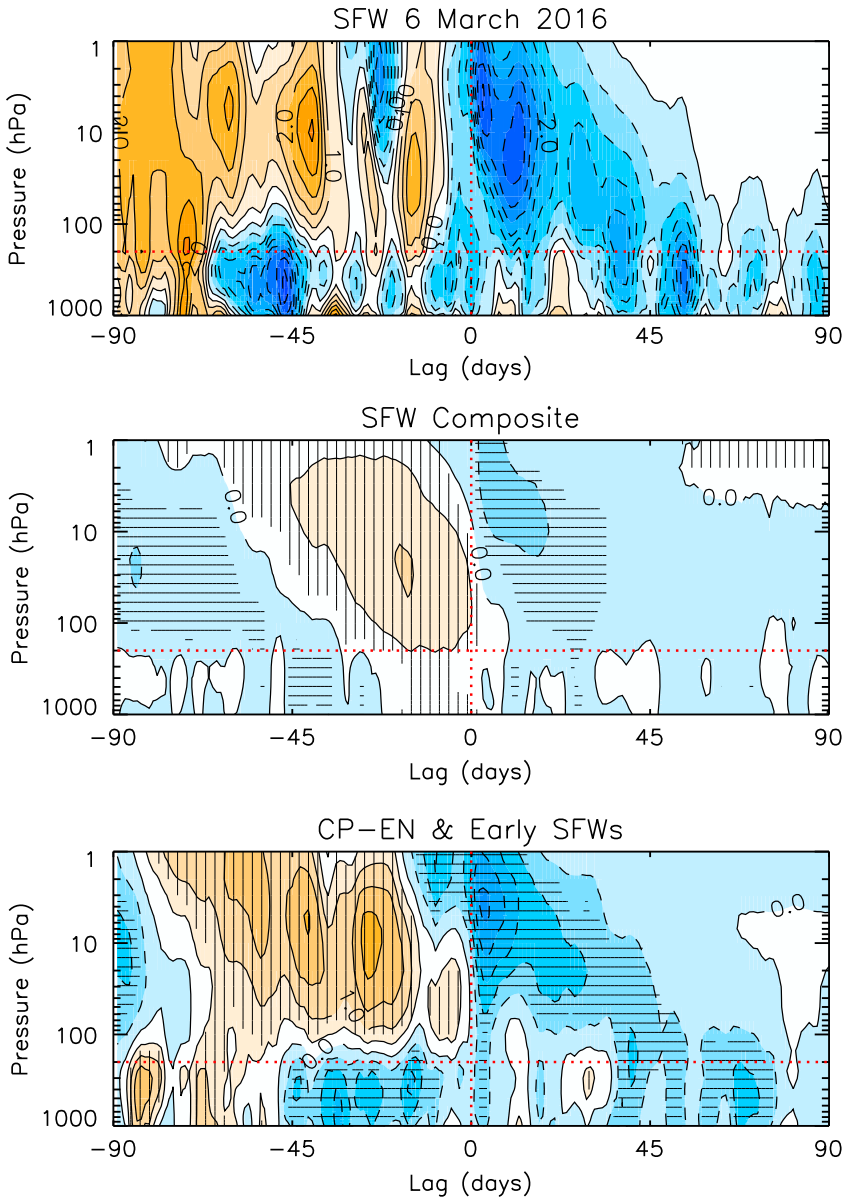


**Figure 4.** Time-height composites of the NAM index (in standard deviation units) for (top) 2016 SFW, (middle) composite of all SFWs in the 1957–2015 period, and (bottom) composite of early SFWs during CP-EN winters (March 1978, 1980, 1988, and 2005, see text for details). Solid (dashed) lines denote positive (negative) NAM values. The abscissa denotes days relative to the SFW onset date. The red horizontal line highlights the 200 hPa pressure level (approximately the extratropical tropopause). Contours interval is 0.5. In Figure 4 (middle and bottom), horizontal (vertical) hatched areas indicate negative (positive) anomalies that are statistically significant at the 90% confidence level.

NAE responses to EN15/16 against the composites for EP-EN and CP-EN events with early SFWs reveals that EN15/16 resembled CP-EN events (Figure 5, bottom row). We note that CP-EN winters without early SFWs and all winters with early SFWs show weaker signatures (not shown). This stresses a CP-EN-like response of EN15/16 and provides evidence of tropospheric effects over Europe following CP-EN events that are accompanied by early SFWs.

## 4. Summary and Conclusions

We explore the strong EN15/16 and provide evidence of its exceptional nature, both in terms of its magnitude and complex behavior, with characteristics of both EP-EN and CP-EN events. Our results indicate that, despite

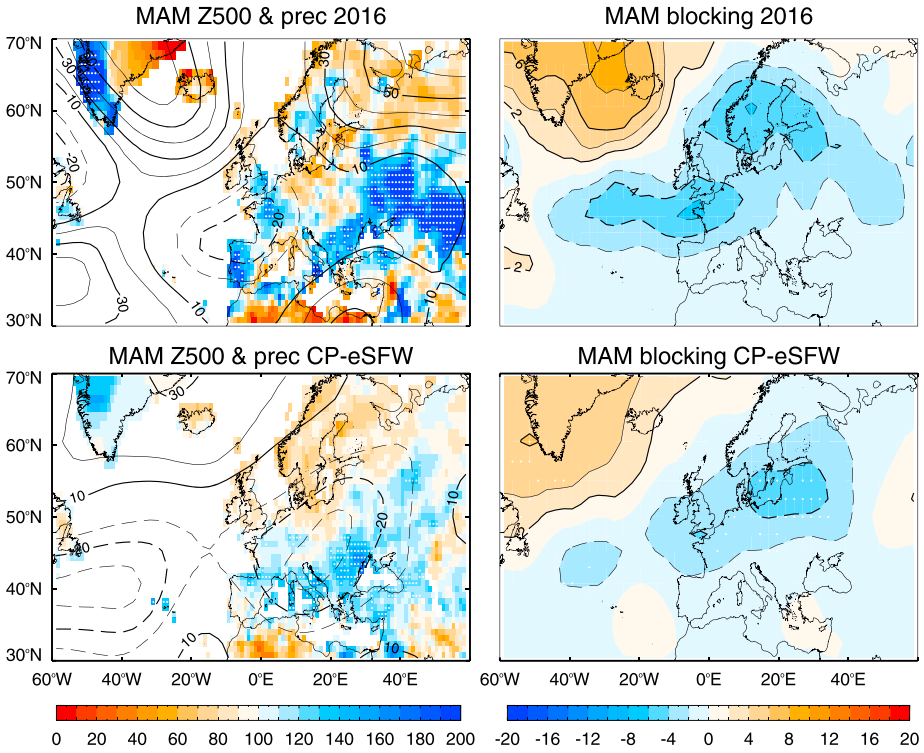


**Figure 5.** Spring (March to May) anomalies of (left column) geopotential height at 500 hPa (contours, gpm) and liquid precipitation over land (shading, in % of totals) and (right column) blocking frequency anomalies (in % of spring days) for (top row) 2016. Stippling indicates seasonal precipitation values that are above the 95th percentile of the local 1981–2010 distribution. (bottom row) The composite of CP-EN winters with early SFWs. In Figure 5 (bottom row), stippling highlights seasonal precipitation (blocking frequency) departures that are significantly larger than (different from) those expected from the climatology at the 90% confidence level.

being cataloged as an EP-EN (N3 = 2.2 SD), EN15/16 showed several signatures that are characteristic of CP-EN events, leading to an unusual event on the observational record (last 59 years). This is supported by the following conclusions.

1. EN15/16 was the strongest CP-EN to date, with N4 = 1.8 SD, which exceeded by 0.3 SD the previous largest CP-EN of 2009–2010. The SSTAs over the equatorial Pacific crossed the dateline toward the west and were spatially more homogeneous than in typical EP-EN events.
2. In the NH polar stratosphere, EN15/16 evidenced CP-EN-like teleconnection signatures. A weakened Aleutian low in early winter and less upward propagation of planetary waves toward the stratosphere led to a midwinter polar cooling. This is similar to teleconnections reported for CP-EN winters without SSWs [*Iza and Calvo*, 2015] and opposite of those associated with EP-EN [e.g., *García-Herrera et al*., 2006].
3. EN15/16 winter was characterized by a lack of SSWs, despite SSWs frequently occur during EP-EN winters [*Butler and Polvani*, 2011]. Instead, EN15/16 winter displayed an extremely early SFW on 6 March leading to a weakening of the polar vortex in March. Even though the behavior of early SFWs and SSWs might be similar [*Hu et al*., 2014b], and thus EP-EN events could also favor early SFWs, our results do not support such relationship in the observational record. In contrast, we find a tendency for CP-EN winters to concur with extremely early SFWs.
4. Similar to CP-EN events with early SFWs, the 2016 SFW displayed a strong stratosphere-troposphere coupling and negative NAM values in the troposphere for several weeks. Accordingly, there were anomalous conditions over the NAE region during spring, which were timely with the downward propagation of the NAM signal. The occurrence of blocking activity over Greenland increased, the storm tracks shifted southward, and the above-normal precipitation occurred over southern Europe and the Mediterranean.

Our results have important implications for surface climate. As early SFWs can display strong stratosphere-troposphere coupling signatures, they are expected to play a mediating role in the tropospheric impacts of

EN, similar to what has been reported for SSWs. In fact, we provide the first evidence that, when accompanied by early SFWs, CP-EN events have notable effects over the NAE sector in late winter and spring.

Finally, our results bring the question of whether or not the complex behavior of EN15/16 was related to the intensity of the event. Other studies have also reported a different response to very strong EN events compared to moderate ones [*Toniazzo and Scaife*, 2006; *Rao and Ren*, 2016]. Given the short length of stratospheric observations, this topic could be better explored in long model simulations with a well-resolved stratosphere.

**Acknowledgments**
We acknowledge the ECMWF for providing ERA-40 and ERA-Interim reanalysis data (http://apps.ecmwf.int/datasets/), the Global Precipitation Climatology Centre for the precipitation data (ftp://ftp-anon.dwd.de/pub/data/gpcc/html/download_gate.html), and the Met Office Hadley Centre for the HadISST1 data (http://www.metoffice.gov.uk/hadobs/hadisst/data/download.html). We thank Kate Willett and an anonymous reviewer for their helpful comments. This work was supported by the Spanish Ministry of Economy and Competitiveness through the PALEOSTRAT (CGL2015-69699-R) project and the European Project 603557-STRATOCLIM under program FP7-ENV.2013.6.1-2. F.M. Palmeiro was funded by grant BES-2013-063906.

## References

Ashok, K., S. K. Behera, S. A. Rao, H. Weng, and T. Yamagata (2007), El Niño Modoki and its possible teleconnection, *J. Geophys. Res.*, *112*, C11007, doi:10.1029/2006JC003798.

Ayarzagüena, B., and E. Serrano (2009), Monthly characterization of the tropospheric circulation over the Euro-Atlantic area in relation with the timing of stratospheric final warmings, *J. Clim.*, *22*(23), 6313–6324, doi:10.1175/2009JCLI2913.1.

Baldwin, M. P., and T. J. Dunkerton (2001), Stratospheric harbingers of anomalous weather regimes, *Science*, *294*(5542), 581–584, doi:10.1126/science.1063315.

Barriopedro, D., and N. Calvo (2014), On the relationship between ENSO, stratospheric sudden warmings, and blocking, *J. Clim.*, *27*, 4704–4720, doi:10.1175/JCLI-D-13-00770.1.

Barriopedro, D., R. García-Herrera, and R. M. Trigo (2010), Application of blocking diagnosis methods to general circulation models. Part I: A novel detection scheme, *Clim. Dyn.*, *35*, 1373–1391, doi:10.1007/s00382-010-0767-5.

Bell, C. J., L. J. Gray, A. J. Charlton-Perez, M. M. Joshi, and A. A. Scaife (2009), Stratospheric communication of El Niño teleconnections to European winter, *J. Clim.*, *22*, 4083–4096, doi:10.1175/2009JCLI2717.1.

Black, R. X., B. A. McDaniel, and W. A. Robinson (2006), Stratosphere-troposphere coupling during spring onset, *J. Clim.*, *19*(19), 4891–4901, doi:10.1175/JCLI3907.1.

Butler, A. H., and L. M. Polvani (2011), El Niño, La Niña, and stratospheric sudden warmings: A reevaluation in light of the observational record, *Geophys. Res. Lett.*, *38*, L13807, doi:10.1029/2011GL048084.

Cagnazzo, C., and E. Manzini (2009), Impact of the stratosphere on the winter tropospheric teleconnections between ENSO and the North Atlantic and European region, *J. Clim.*, *22*, 1223–1238, doi:10.1175/2008JCLI2549.1.

Charlton, A. J., and L. M. Polvani (2007), A new look at stratospheric sudden warmings. Part I: Climatology and modeling benchmarks, *J. Clim.*, *20*, 449–469, doi:10.1175/JCLI3996.1.

Davini, P., C. Cagnazzo, and J. A. Anstey (2014), A blocking view of the stratosphere-troposphere coupling, *J. Geophys. Res. Atmos.*, *119*, 11,100–11,115, doi:10.1002/2014JD021703.

Dee, D. P., et al. (2011), The ERA-Interim reanalysis: configuration and performance of the data assimilation system, *Q. J. R. Meteorol. Soc.*, *137*, 553–597, doi:10.1002/qj.828.

García-Herrera, R., N. Calvo, R. R. Garcia, and M. A. Giorgetta (2006), Propagation of ENSO temperature signals into the middle atmosphere: A comparison of two general circulation models and ERA-40 reanalysis data, *J. Geophys. Res.*, *111*, D06101, doi:10.1029/2005JD006061.

Garfinkel, C. I., M. M. Hurwitz, D. W. Waugh, and A. H. Butler (2013), Are the teleconnections of Central Pacific and Eastern Pacific El Niño distinct in boreal wintertime?, *Clim. Dyn.*, *41*, 1835–1852, doi:10.1007/s00382-012-1570-2.

Gimeno, L., R. Nieto, and R. M. Trigo (2007), Decay of the Northern Hemisphere stratospheric polar vortex and the occurrence of cut-off low systems: An exploratory study, *Meteorol. Atmos. Phys.*, *96*(1–2), 21–28, doi:10.1007/s00703-006-0218-3.

Hardiman, S. C., et al. (2011), Improved predictability of the troposphere using stratospheric final warmings, *J. Geophys. Res.*, *116*, D18113, doi:10.1029/2011JD015914.

Hu, J. G., R. Ren, and H. Xu (2014a), Occurrence of winter stratospheric sudden warming events and the seasonal timing of spring stratospheric final warming, *J. Atmos. Sci.*, *27*, 2319–2334, doi:10.1175/JAS-D-13-0349.1.

Hu, J. G., R. C. Ren, Y. Y. Yu, and X. HaiMing (2014b), The boreal spring stratospheric final warming and its interannual and interdecadal variability, *Sci. China Earth Sci.*, *57*, 710–718, doi:10.1007/s11430-013-4699-x.

Ineson, S., and A. A. Scaife (2009), The role of the stratosphere in the European climate response to El Niño, *Nat. Geosci.*, *2*, 32–36, doi:10.1038/ngeo381.

Iza, M., and N. Calvo (2015), Role of stratospheric sudden warmings on the response to central Pacific El Niño, *Geophys. Res. Lett.*, *42*, 2482–2489, doi:10.1002/2014GL062935.

L'Heureux, M. L., et al. (2016), Observing and predicting the 2015-16 El Niño, *Bull. Am. Meteorol. Soc.*, in press.

Manzini, E., M. A. Giorgetta, M. Esch, L. Kornblueh, and E. Roeckner (2006), The influence of sea surface temperatures on the Northern winter stratosphere: Ensemble simulations with the MAECHAM5 model, *J. Clim.*, *19*, 3863–3882, doi:10.1175/JCLI3826.1.

Matsuno, T. (1971), A dynamical model of the stratospheric sudden warming, *J. Atmos. Sci.*, *28*, 1479–1494.

Newman, P. A., L. Coy, S. Pawson, and L. R. Lait (2016), The anomalous change in the QBO in 2015–2016, *Geophys. Res. Lett.*, *44*, 8791–8797, doi:10.1002/2016GL070373.

Osprey, S. M., N. Butchart, J. R. Knight, A. A. Scaife, K. Hamilton, J. A. Anstey, and C. Zhang (2016), An unexpected disruption of the atmospheric quasi-biennial oscillation, *Science*, *353*(6306), 1424–1427, doi:10.1126/science.aah4156.

Palmeiro, F. M., D. Barriopedro, R. García-Herrera, and N. Calvo (2015), Comparing sudden stratospheric warming definitions in reanalysis data, *J. Clim.*, *28*, 6823–6840, doi:10.1175/JCLI-D-15-0004.1.

Parker, D. E., K. M. Willet, R. Allan, C. Schreck, and D. S. Arndt (2015), The 2015/16 El Niño compared with other recent events [in "State of the Climate in 2015"], *Bull. Am. Meteorol. Soc.*, *97*(8), S55–S56.

Rao, J., and R. Ren (2016), Asymmetry and nonlinearity of the influence of ENSO on the northern winter stratosphere: 1. Observations, *J. Geophys. Res. Atmos.*, *121*, 9000–9016, doi:10.1002/2015JD024520.

Rayner, N. A., D. E. Parker, E. B. Horton, C. K. Folland, L. V. Alexander, D. P. Rowell, E. C. Kent, and A. Kaplan (2003), Global analyses of sea surface temperature, sea ice, and night marine air temperature since the late nineteenth century, *J. Geophys. Res.*, *108*(D14), 4407, doi:10.1029/2002JD002670.

Ren, R., and J. Hu (2014), An emerging precursor signal in the stratosphere in recent decades for the Indian summer monsoon onset, *Geophys. Res. Lett.*, *41*, 7391–7396, doi:10.1002/2014GL061633.

Schneider, U., A. Becker, P. Finger, A. Meyer-Christoffer, B. Rudolf, and M. Ziese (2015a), GPCC full data reanalysis version 7.0 at 1.0°: Monthly land-surface precipitation from rain-gauges built on GTS-based and historic data, doi:10.5676/DWD_GPCC/FD_M_V7_100.

Schneider, U., A. Becker, P. Finger, A. Meyer-Christoffer, B. Rudolf, and M. Ziese (2015b), GPCC monitoring product: Near real-time monthly land-surface precipitation from rain-gauges based on SYNOP and CLIMAT data, doi:10.5676/DWD_GPCC/MP_M_V5_100; 10.5676/DWD_GPCC/MP_M_V5_100.

Sousa, P. M., D. Barriopedro, R. M. Trigo, A. M. Ramos, R. Nieto, L. Gimeno, K. F. Turkman, and M. L. R. Liberato (2016), Impact of Euro-Atlantic blocking patterns in Iberia precipitation using a novel high resolution dataset, *Clim. Dyn.*, *46*(7), 2573–2591, doi:10.1007/s00382-015-2718-7.

Thompson, D. W. J., and J. M. Wallace (1998), The Arctic Oscillation signature in the wintertime geopotential height and temperature fields, *Geophys. Res. Lett.*, *25*(9), 1297–1300, doi:10.1029/98GL00950.

Toniazzo, T., and A. A. Scaife (2006), The influence of ENSO on winter North Atlantic climate, *Geophys. Res. Lett.*, *33*, L24704, doi:10.1029/2006GL027881.

Uppala, S. M., et al. (2005), The ERA-40 re-analysis, *Q. J. R. Meteorol. Soc.*, *131*(612), 2961–3012, doi:10.1256/qj.04.176.

Woollings, T., A. Hannachi, and B. Hoskins (2010), Variability of the North Atlantic eddy-driven jet stream, *Q. J. R. Meteorol. Soc.*, *136*, 856–868, doi:10.1002/qj.625.

Zubiaurre, I., and N. Calvo (2012), The El Niño-Southern Oscillation (ENSO) Modoki signal in the stratosphere, *J. Geophys. Res.*, *117*, D04104, doi:10.1029/2011JD016690.